Accurate Calculation and Sensitivity Analysis of Leakage Inductance of High-Frequency Transformer With Litz Wire Winding

Ke Zhang, Wu Chen, *Senior Member, IEEE*, Xiaopeng Cao, Pengpeng Pan, Syed Waqar Azeem, Guangyao Qiao, and Fujin Deng, *Senior Member, IEEE*

***Abstract*—Leakage inductance is an important parameter in a high-frequency transformer for its influence on power transmission performance and the soft switching of converters. Nowadays, Litz wire is widely used to control winding loss and reach high efficiency. However, it is not an easy task to accurately calculate its leakage inductance. This article presents a detailed model of leakage energy in Litz wire, and proposes an accurate closed-form expression for calculating the leakage inductance in a high-frequency transformer. The skin effect and the proximity effect of Litz wire are taken into account in two-dimensional polar coordinates, and the filling factor of Litz wire is also considered. A global sensitivity analysis is performed to assess the influence of each parameter on the overall leakage inductance. Finally, two transformer prototypes are made to verify the accuracy of the proposed analytical expression.**

***Index Terms*—Analytical method, high-frequency transformer, leakage inductance, Litz wire, sensitivity analysis.**

NOMENCLATURE

d_{ins}	Interwinding insulation distance.
$d_{ins1/2}$	Insulation distance between winding layers of primary and secondary windings, respectively.
$d_{1/2}$	Winding layer thickness of primary and secondary windings, respectively.
d_{ins_core}	Distance between winding and core.
h_w	Winding height.
h_c	Window height.
l_{mean}	Mean magnetic path length.
l_g	Mean magnetic path length of insulation inter winding.
$l_{1/2}$	Mean magnetic path length of primary and secondary windings.
$m_{1/2}$	Number of layers of primary and secondary winding, respectively.
$I_{1/2}$	RMS value of current in primary and secondary windings, respectively.
I_p	Peak value of the conducting current in a Litz bundle.
δ	Skin depth.
Δ	Penetration ratio.
N	Number of turns of Litz bundle per layer.
D_{Litz}, R_{Litz}	Diameter and radius of Litz bundle.
D_s, R_s	Diameter and ratius of Litz strand.
R_m	Magnetic Reynolds number.
H_{int}	Internal leakage field in Litz bundle.
H_{ext}	External leakage field across the window.
H_{stage}	Averaged magnetic field strength excited by conductors in one single layer.
S_i	First order effect index (main effect index).
S_T	Total effect index.
β	Filling factor of Litz wire.
γ_1	Skin factor.
γ_2	Proximity factor.
$J_\alpha(x)$	Bessel function of the first kind.

Manuscript received January 30, 2019; revised April 23, 2019 and July 1, 2019; accepted August 13, 2019. Date of publication August 20, 2019; date of current version January 10, 2020. This work was supported in part by the National Key R&D Program of China under Grant 2017YFB0903905 and in part by the Natural Science Foundation of China under Grant 51922028. Recommended for publication by Associate Editor M. Duffy. *(Corresponding author: Wu Chen.)*

K. Zhang, W. Chen, P. Pan, and S. W. Azeem are with the Center for Advanced Power-Conversion Technology and Equipment, School of Electrical Engineering, Southeast University, Nanjing 210096, China (e-mail: ke_zhang@seu.edu.cn; chenwu@seu.edu.cn; 2727101609@qq.com; waqar_azeem11@hotmail.com).

X. Cao is with the State Grid Chengdu Power Supply Company, Chengdu 610000, China (e-mail: 1092604443@qq.com).

G. Qiao is with the State Key Laboratory of Advanced Power Transmission Technology, Global Energy Interconnection Research Institute, Beijing 102209, China (e-mail: gyqiao@126.com).

F. Deng is with the School of Electrical Engineering, Southeast University, Nanjing 210096, China, and also with the Jiangsu Key Laboratory of Smart Grid Technology and Equipment, Nanjing 2120096, China (e-mail: fdeng@seu.edu.cn).

Color versions of one or more of the figures in this article are available online at http://ieeexplore.ieee.org.

Digital Object Identifier 10.1109/TPEL.2019.2936523

I. INTRODUCTION

POWER electronic transformers (PETs) have received growing attention for its ability to fulfill the function of grid power flow control, power quality management, renewable energy interfacing, and so forth. As a key component of a PET, a high-frequency transformer has the advantages of reducing transformer weight, volume, and increasing power density compared with a bulky 50/60 Hz transformer [1], [2]. The resonant converters or dual active bridge (DAB) converters are mostly employed in the dc–dc stage of a PET, in which the series inductors are required to achieve desirable power transmission and soft-switching characteristics [3]–[5]. To achieve higher

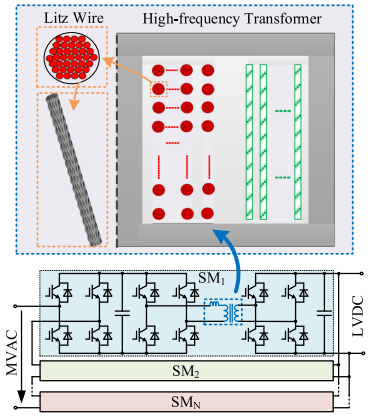

Fig. 1. PET topology with a high-frequency transformer.

power density and lower cost, the leakage inductor of the high-frequency transformer is usually taken as the series inductor for a resonant converter or DAB converter and, thus, no extra inductor is required. This supports application scenarios of the PETs in many areas, including but not limited to smart distribution grid, railway traction system, and renewable energy system [6]. For instance, as shown in Fig. 1, a PET adopts cascaded H-bridge converters at the medium-voltage ac-grid side and each H-bridge is linked with a DAB converter, which includes an isolation transformer and a series inductor, the mentioned two passive components could be integrated into a high-frequency transformer, as shown in Fig. 1. Multiple DAB converters are connected in parallel at low-voltage side to generate the low-voltage dc output [7]. Therefore, as an important resonant parameter for a resonant converter and an energy transfer component for a DAB converter, a precise calculation and a design of leakage inductance in high frequency is crucial to meet performance requirements [8]. For instance, in converters systems such as PET or input series output parallel converters employing *LC* resonant converters as their submodule, the value of resonant component should be perfectly tuned or the operating frequency will be changed, small frequency discordance between modules could cause unexpected problems, including increased difficulty in designing a control system [9].

Mainly two parts constitute the leakage inductance energy in a transformer: one is stored in a winding conductor and another is stored in an insulation region (including air) [8]. The decline of leakage inductance in high frequency on account of magnetic field unevenness caused by the eddy effect and the proximity effect is neglected in traditional analytical methods [10], [11]. Inspired by Hurley's work [12], Bahmani and Thiringer [1] and Ouyang *et al.* [8] individually made remarkable research on the frequency effect of leakage inductance based on Dowell's one-dimensional (1-D) electromagnetic model, and proposed different but equivalent closed-form expressions to calculate the frequency-dependent leakage inductance in foil winding transformers. The scenario for cross construction of the primary and secondary windings is analyzed in [8] and the expression for a solid round conductor is modified using an area equivalence method in [1]. Considering the edge effect on magnetic field distribution when winding height is lower than core window height, the equivalent magnetic path length is corrected by Rogowski's factor [13], [14], improving calculation accuracy in high-voltage insulation occasion. Besides, research on leakage inductance of a planar transformer (whose winding could be viewed as a special case of foil) has been conducted in [15] and [16].

The development of wide band-gap semiconductor devices pushes the operating frequency into higher range to minimize the size of the magnetic components [19], [20]. In higher operating frequency applications, Litz wire winding, as an alternative to foil winding, is widely implemented to reduce the winding loss and improve efficiency, and its loss characteristic is fully modeled and illustrated in [21] and [22]. As for finite element method, a homogenized model for Litz wire is proposed by Nan and Sullivan [23] and further studied by Meeker [24], reducing the computation cost of finite element analysis (FEA) for a Litz wire winding transformer. Although substantial research has been conducted on the analytical calculation of leakage inductance of transformers using the foil and solid round conductor windings [1], [8], [10]–[18], rather few literature tries to analytically model the leakage inductance of transformer with Litz wire winding [14].

Mogorovic and Dujic adopt an area equivalence method to correct the leakage energy in rectangle Litz wire, providing that one layer of Litz wire is equivalent to a stack of thinner foils [14]. The area equivalence method yields remarkable accuracy in winding loss calculation, but it tends to overestimate the frequency effect on the leakage inductance because it neglects the impact of filling factor in Litz wire. Besides, this equivalence is rather empirical because several correction factors lack solid physical explanation. As a result, a more accurate analytical model of the leakage inductance of transformer with Litz wire winding needs to be studied.

In addition, there are excessive parameters in the analytical expression of leakage inductance. When performing an overall optimization algorithm for a high-frequency transformer with a desired leakage inductance, it will take long computation time if all parameters are taken into consideration. Therefore, the influence of parameters should be analyzed so that those more influential parameters on leakage inductance will be taken as free variables and the other parameters could be fixed, reducing computation time.

The purpose of this article is to propose a closed-form expression for accurately calculating the leakage inductance of a high-frequency transformer implementing a round Litz wire in a a wide frequency range. The proposed method considers the skin and proximity effects in a 2-D electromagnetic field as well as the filling factor of Litz wire winding. Detailed derivation of the proposed ideal model and accurate model are conducted and the application boundary of the two model is analyzed. In addition, a parameter sensitivity analysis is performed to assess which parameters influence the leakage inductance the most.

The remainder of the article is organized as follows. Section II explains the methodology and gives a detailed derivation of the leakage inductance closed-form expression. Section III conducts a Sobol-based global parameter sensitivity analysis and verifies

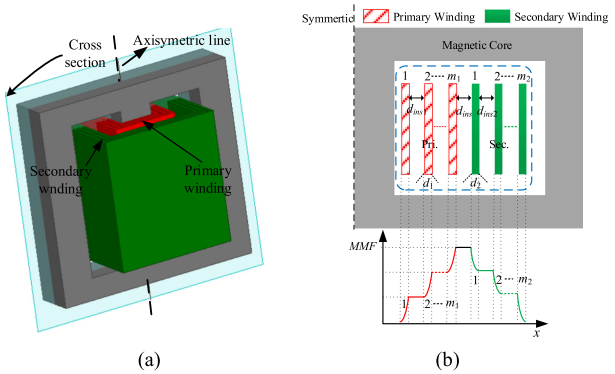

Fig. 2. Transformer structure. (a) Three-dimensional structure. (b) Two-dimensional axisymmetric cross-sectional view along with MMF distribution within core window.

the influence of each parameter in the expression through parameter sweeping. In Section IV, experimental results of the two transformer prototypes are presented. Section V provides a conclusion.

II. Expression Derivation

In this section, the general leakage inductance model of a high-frequency transformer is reviewed at first. An ideal leakage inductance model for Litz wire (assuming the diameter of Litz strand approaching zero) is proposed. After that, considering the strand-level skin effect and proximity effect, an accurate frequency-dependent leakage inductance model is proposed to guarantee high accuracy in a wide frequency range. Finally, the relationship between the ideal model and accurate model is analyzed.

A. General Leakage Inductance Model

The leakage inductance of a transformer represents the magnetic field that leaks from the core and returns through the air rather than linking both windings. If the secondary winding is shorted, the main flux in the core that links both primary and secondary windings will be negligible because the primary and secondary ampere-turns are almost cancelled. Fig. 2 shows an EE type transformer and the magnetic motive force (MMF) distribution in its window. In this condition, the magnetic energy within a transformer window determines the leakage inductance.

1) Energy stored between primary winding and secondary winding (interwinding)

$$W_g = \frac{1}{2}\mu \int_0^{d_{\rm ins}} \left(\frac{m_1 I_1}{h_w}\right)^2 h_w l_g dx = \frac{\mu \cdot l_g d_{\rm ins}}{2h_w} m_1^2 I_1^2 \tag{1}$$

where $d_{\rm ins}$ represents the interwinding insulation distance, l_g stands for the mean magnetic path length of insulation inter winding, h_w is the winding height, m_1 is the number of layers of primary winding, and I_1 is the rms value of current in primary winding (m_2 and I_2 denote their respective values of secondary winding).

2) Energy stored in the winding layers of primary winding and secondary winding (interlayer) [25]

$$\begin{aligned} W_{\rm pri/sec\_ins} &= \sum_{i=1}^{m-1} \frac{1}{2}\mu \int_0^{d_{ins}} \left(i\frac{I}{h_w}\right) h_w l dx \\ &= \frac{\mu l d_{\rm ins}}{12h_w} m(m-1)(2m-1) I^2 \\ m = m_1 \text{ or } m_2,\ d_{\rm ins} &= d_{\rm ins1} \text{ or } d_{\rm ins2},\ l = l_1 \text{ or } l_2, \\ I &= I_1 \text{ or } I_2 \end{aligned} \tag{2}$$

where d_{ins1} and d_{ins2} represent the insulation thickness between the winding layers of primary and secondary windings, respectively (interlayer insulation thickness), and l_1 and l_2 represent the mean magnetic path length of primary and secondary windings, respectively. Note that the leakage magnetic energy stored in the winding insulation layers $W_{\rm pri/sec\_ins}$ has two parts: energy stored in primary winding insulation layers $W_{\rm pri\_ins}$, and energy stored in secondary winding insulation layers $W_{\rm sec\_ins}$. For example, when calculating $W_{\rm pri\_ins}$, the quantities m_1, d_{ins1}, l_1, and I_1 ought to be used.

3) Energy stored in the winding conductors (within conductor) [25]

$$\begin{aligned} W_{\rm pri/sec} &= \frac{\mu l \delta}{12h_w} m\left[\left(4m^2-1\right)F_1 - 2\left(m^2-1\right)F_2\right] I^2 \\ F_1 &= \frac{\sin h(2\Delta) - \sin(2\Delta)}{\cos h(2\Delta) - \cos(2\Delta)},\ F_2 = \frac{\sin h(\Delta) - \sin(\Delta)}{\cos\ h(\Delta) - \cos(\Delta)} \\ \Delta &= \frac{d}{\delta},\ d = d_1 \text{ or } d_2, m = m_1 \text{ or} m_2,\ I = I_1 \text{ or } I_2 \end{aligned} \tag{3}$$

where d_1 and d_2 represent the thickness of a conductor in primary and secondary windings, respectively, and δ is the skin depth. The total leakage inductance can be represented as follows:

$$L_\delta = \frac{2}{{I_1}^2}\left(W_g + W_{\rm pri} + W_{\rm sec} + W_{\rm pri\_ins} + W_{\rm sec\_ins}\right). \tag{4}$$

This analytical expression yields high accuracy in a transformer implementing a foil or solid round conductor (equivalent to foil). However, a high-frequency transformer usually adopts Litz wire as its winding conductor for the loss optimization. In [14], a layer of the rectangle Litz wire conductor is equivalent to a stack of thinner foils and then (3) can be used for the leakage inductance calculation. However, this equivalence method would overestimate the frequency effect on the leakage inductance because it neglects the impact of filling factor in Litz wire; besides, several correction factors lack solid physical explanation. Moreover, round Litz wire, including multiple twisted wire, is most commonly implemented in practical application. Therefore, a comprehensive model of round Litz wire should be built to precisely calculate its leakage inductance.

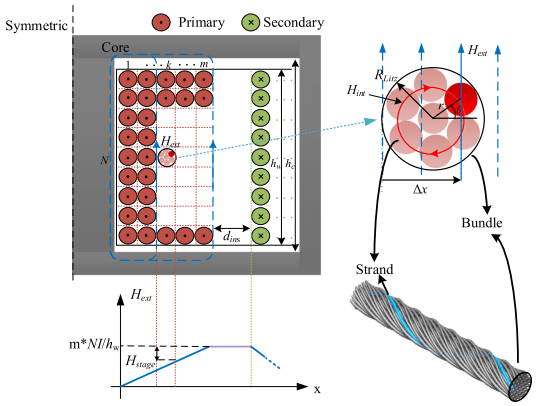

Fig. 3. Leakage field distribution in core window of a Litz wire winding transformer.

B. Ideal Litz Wire Leakage Model

Before analysis, there are two assumptions.

Assumption A) Ideal Litz wire is twisted by the infinite strands of enameled round thin conductor and the diameter of each strand approaches zero, thus strand-level skin effect and proximity effect can be neglected.

Assumption B) Each strand is waved along the entire divided conductor in such a way that all wires successively pass through all points at the cross section of the conductor, it guarantees that each strand shares equal current. [26]

Fig. 3 shows a structure and leakage field distribution of the proposed ideal model, each strand is submitted to not only an internal annular leakage field H_{int} excited by current in other strands in the bundle, but also an external leakage field H_{ext} in the *Y*-direction in core window [22]. Then the magnetic field across the Litz wire is determined as follows:

$$\begin{aligned}\overrightarrow{H_{\text{bundle}}} &= \overrightarrow{H_{\text{int}}} + \overrightarrow{H_{\text{ext}}} \\ &= [H_{\text{ext}} + H_{\text{int}}\sin(\theta)]\ \vec{y} + H_{\text{int}}\cos(\theta)\ \vec{x}\,. \end{aligned} \tag{5}$$

According to the distribution of external field H_{ext} across the window shown in Fig. 3, the field imposed on position Δx of the *k*th layer is given by

$$\begin{aligned} H_{\text{ext}}(k,\Delta x) &= (k-1)H_{\text{stage}} + \frac{\Delta x}{D_{\text{Litz}}}H_{\text{stage}} \\ H_{\text{stage}}&\frac{NI_P}{h_w} \end{aligned} \tag{6}$$

where H_{stage} represents the averaged magnetic field strength excited by conductors in one single layer, *N* is the number of Litz bundles per layer, I_p is the peak value of the sinusoidal conducting current in a Litz bundle, D_{Litz} represents the diameter of Litz bundle, and h_w is the winding height.

In the occasion where the winding height h_w is much smaller than the window height h_c, one can use Rogowski's factor to compensate the effective winding height, as shown in (7) [13], where d_{ins} is the main insulation distance between primary and secondary windings, and d_{ins1} and d_{ins2} stand for the insulation distance between the winding layers in primary and secondary windings, respectively.

$$\begin{aligned} p &= 1 \\ &- \frac{d_{\text{ins}} + (m_1+m_2)D_{\text{Litz}} + (m_1-1)d_{\text{ins1}} + (m_2-1)d_{\text{ins2}}}{\lambda h_w^2} \\ h'_w &= \frac{h_w}{p}. \end{aligned} \tag{7}$$

In order to describe the magnetic field strength vector in the 2-D polar coordinates, Δx can be rewritten as

$$\Delta x = R_{\text{Litz}} + r\cos(\theta) \tag{8}$$

where R_{Litz} represents the radius of Litz bundle, as a result, the modified external field can be represented as

$$H_{\text{ext}} = \left(k - \frac{1}{2} + \frac{r}{R_{\text{Litz}}}\cdot\frac{\cos(\theta)}{2}\right)H_{\text{stage}}. \tag{9}$$

According to Ampere's law, the internal magnetic field in the Litz bundle is given by

$$H_{\text{int}} = \frac{I_p}{2\pi {R_{\text{Litz}}}^2}r. \tag{10}$$

Combining (5), (9), and (10), one can obtain the expression for the leakage magnetic field in ideal Litz wire

$$\begin{aligned}\overrightarrow{H_{\text{total}}} = &\left[\left(\left(k - \frac{1}{2} + \frac{r}{R_{\text{Litz}}}\frac{\cos(\theta)}{2}H_{\text{stage}}\right)\right.\right. \\ &\left.\left. + \left(\frac{I_p}{2\pi R_{\text{Litz}}^2}r\right)\sin(\theta)\right]\right. \\ &\vec{y} + \left(\frac{I_p}{2\pi R_{\text{Litz}}^2}r\right)\cos(\theta)\ \vec{x}\,. \end{aligned} \tag{11}$$

The leakage energy in a single bundle is determined by

$$\begin{aligned} W_{\text{litz}(i)} &= \frac{1}{2}\mu\int H^2 dV \\ &= \frac{1}{4}\mu_0\int_0^{2\pi}\int_0^{R_{\text{Litz}}} {H_{\text{total}}}^2 r dr d\theta \cdot l_{\text{mean}}. \end{aligned} \tag{12}$$

As shown in Fig. 1, there are *m* layers of winding and *N* turns of Litz wire in each layer. Substituting (11) into (12), one can obtain the ideal total leakage energy stored in the winding

$$\begin{aligned} &W_{\text{Litz}(i)} \\ &= \frac{\mu_0 l_{\text{mean}}}{4}\left(\frac{\pi(16k^2-16k+5)H_{\text{stage}}^2 R_{\text{Litz}}^2}{8} + \frac{I_p^2}{4\pi}\right) \\ &W_{\text{pri/sec\_Litz}(i)} = \sum_{k=1}^{m} N W_{\text{Litz}}. \end{aligned} \tag{13}$$

C. Accurate Litz Wire Leakage Model

Actual Litz wire is formed by twisting and transposing a plurality of surface-insulated round conductors with an outer diameter of around 0.08–0.2 mm. Although the winding process

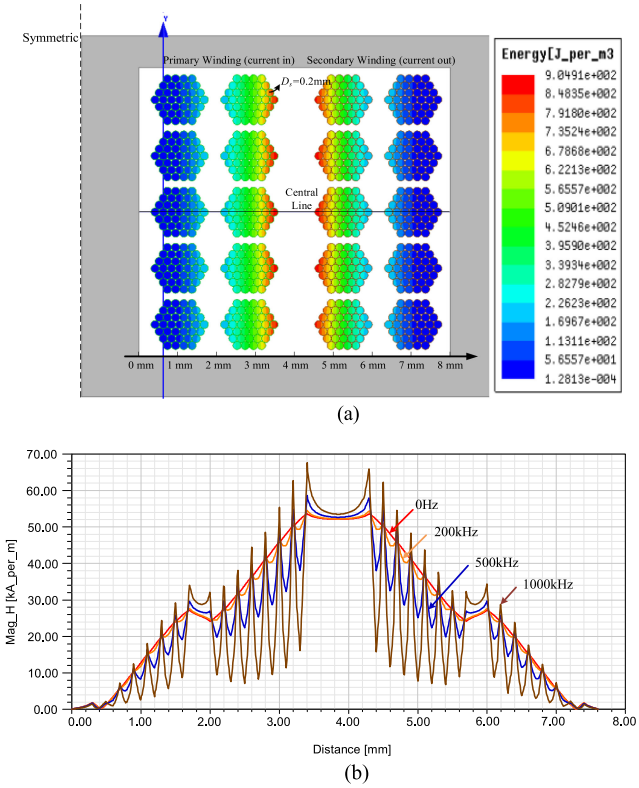

Fig. 4. Unevenness of leakage field distribution within transformer window at different frequencies. (a) Winding structure and leakage energy distribution. (b) FEA results of magnetic field strength along the *x*-axis of the central line in (a).

enables the current in the Litz bundle to be evenly distributed in strands, eliminating the bundle-level skin effect and proximity effect, each strand with finite diameter is still affected by high-frequency effect, forcing the magnetic field distribution inside each strand to be distorted. Fig. 4 shows the unevenness of leakage field distribution within a transformer window at different frequencies. In Fig. 4(a), the FEA of transformer leakage energy using the Litz bundle composed of 37 strands with a strand diameter of 0.2 mm is performed using *Maxwell 16.0*. There are two layers of Litz winding with five turns of the Litz bundle in each layer in both primary and secondary sides. The current in each strand is assigned as 1 A in primary winding (and -1 A in secondary winding) to guarantee the *Assumption B)* in the proposed ideal model of Section II-B (each strand shares the same current). Fig. 4(b) shows the FEA results of the leakage magnetic field strength H along the x-axis of the central line drawn in Fig. 4(a).

It can be seen that the unevenness of magnetic field distribution with the increase of frequency attenuates the leakage energy stored in conductor. This invalidates the *Assumption A)* in the proposed ideal model of Section II-B. Consequently, the strand-level skin effect and proximity effect should be taken into account in accurate modeling. In this condition, the Litz bundle could be viewed as the superposition of a set of homogeneous strands satisfying the *Assumption B)*. In addition, the strand-level skin effect and proximity effect can be separately considered based on the orthogonality between them [27].

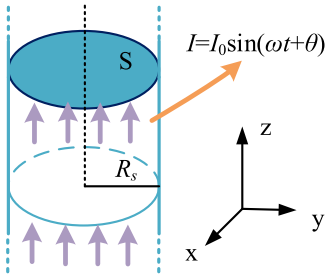

Fig. 5. Single round strand conducting a time-varying current.

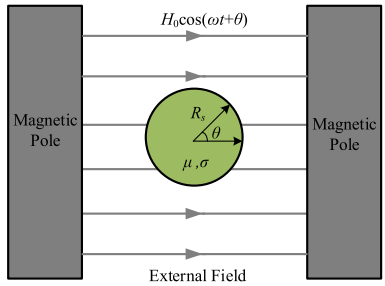

Fig. 6. Single round conductor submitted to a time-varying traverse magnetic field.

1) Skin Effect in a Single Round Strand: As shown in Fig. 5, suppose a cylinder conductor flowing a sinusoidal current with amplitude I_0 and angular frequency ω, then the magnetic field can be derived from the Maxwell equation in the quasistatic field as follows:

$$\frac{d^2H_Z}{dr^2}+\frac{1}{r}\frac{dH_Z}{dr}+k^2H_Z=0$$
$$K=\frac{1+j}{\delta}. \tag{14}$$

The magnetic field distribution in Fig. 5 is obtained by solving the above-mentioned first-order Bessel equation, with its result [28] presented in (15). $J_\alpha(x)$ is the Bessel function of the first kind.

$$H_z(r,f)=\frac{I_0}{2\lambda R_s}\cdot\frac{J_1(kr)}{J_1(kR_s)}$$
$$J_\alpha(x)=\sum_{m=0}^{\infty}\frac{(-1)^m}{m!\Gamma(m+\alpha+1)}\left(\frac{x}{2}\right)^{2m+\alpha}. \tag{15}$$

2) Proximity Effect in Single Strand: As shown in Fig. 6, suppose a cylinder conductor is submitted to a traverse time-varying magnetic field with amplitude H_0 and angular frequency ω.

Perry and Jones [29] have done a detailed analysis of this condition and presented the expression for two orthogonal decoupled magnetic field strength inside the conductor. The derivation is complex and only results are presented

here

$$H_r = \mathrm{Re}\left\{\frac{H_0(1+\frac{R'^2}{R_s{}^2})RJ_1(\frac{R_s\sqrt{j}}{\delta})\cos(\theta)}{rJ_1\sqrt{jR_m}}\right\}$$

$$H_\theta = \mathrm{Re}\left\{\frac{-H_0\left(1+\frac{R'^2}{R_s{}^2}\right)\left[\sqrt{jR_m}J_0\left(\frac{r\sqrt{j}}{\delta}\right)-\left(\frac{R_s}{r}\right)J_1\left(\frac{r\sqrt{j}}{\delta}\right)\right]\sin(\theta)}{J_1\sqrt{jR_m}}\right\}. \tag{16}$$

The definition of parameters in (16) are shown in (17), where R_m is called magnetic Reynolds number, μ_0 is the magnetic permeability of the conducting material (copper), and $J_\alpha(x)$ is the Bessel function of the first kind, with its expression shown in (15).

$$R'^2 = R_s{}^2\left[\frac{2J_1(\sqrt{jR_m})}{J_0(\sqrt{jR_m})}-1\right]$$
$$R_m = \left(\frac{R_s}{\delta}\right)^2,\ \delta = \sqrt{\frac{2}{\omega\mu_0\sigma}}. \tag{17}$$

Since all the strands in the Litz wire bundle pass through each position on the cross section of the bundle, the current in the Litz bundle is equally distributed in each strand, the Litz bundle can be viewed as a combination of multiple individual round conductors with the strand-level skin and the proximity effect. Therefore, the magnetic field energy of the entire Litz bundle can be corrected by the two strand-level normalization factor (skin factor γ_1 and proximity factor γ_2) defined in (18) to describe the decrease of magnetic energy in high frequency.

$$\gamma_1 = \frac{\frac{1}{2}\int H_z{}^2(r,f)dV}{\frac{1}{2}\int H_z{}^2(r,0)dV}$$
$$\gamma_2 = \frac{\frac{1}{2}\int\left[H_r^2(r,\theta,f)+H_\theta^2(r,\theta,f)\right]dV}{\frac{1}{2}\int\left[H_r^2(r,\theta,0)+H_\theta^2(r,\theta,0)\right]dV}. \tag{18}$$

The quantities in (18) are calculated using MATLAB, in which "*r*" and "θ " are defined as symbolic variables, "*f*" is defined as a 1-D array. The Bessel function can be represented by function "*besselj*" and the double integrals are calculated using nested functions "*int*" in MATLAB. The frequency characteristics of the two coefficients are shown in Fig. 7 (strand diameter: 0.1 mm). It can be seen that the values of both factors decrease with the increase of frequency, representing that the leakage energy within Litz strand declines. Moreover, the proximity effect has a much stronger influence on leakage energy compared with skin effect when skin depth exceeds strand diameter.

The frequency-dependent leakage magnetic energy of the Litz wire conductor can be obtained from (13) by multiplying γ_1 and γ_2, respectively. It is noticeable that due to the imperfect filling of multiple strands and inner insulation layer, actual Litz wire has a filling factor β around 0.4–0.6. Only the conducting parts made of copper is susceptible to the skin effect and proximity effect. As a result, the frequency-dependent part and constant part (air, insulation) inside the Litz bundle should be calculated

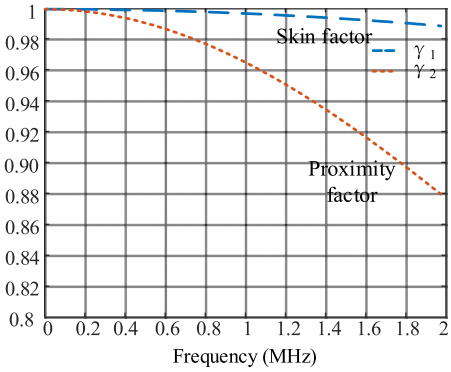

Fig. 7. Influences of skin effect and proximity effect on leakage energy within a Litz conductor.

separately and added together.

$$W_{\mathrm{Litz\_}cu} = \frac{\mu_0 l_{\mathrm{mean}}}{4}\left(\frac{\pi(16k^2-16k+5)H_{\mathrm{stage}}^2R_{\mathrm{Litz}}^2}{8}\cdot\gamma_2 + \frac{I_p^2}{4\pi}\cdot\gamma_1\right)\cdot\beta$$
$$W_{\mathrm{Litz\_}ct} = \frac{\mu_0 l_{\mathrm{mean}}}{4}\left(\frac{\pi(16k^2-16k+5)H_{\mathrm{stage}}^2R_{\mathrm{Litz}}^2}{8} + \frac{I_p^2}{4\pi}\right)\cdot(1-\beta)$$
$$W_{\mathrm{Litz}} = W_{\mathrm{Litz\_}cu} + W_{\mathrm{Litz\_}ct}$$
$$W_{\mathrm{pri/sec\_Litz}} = \sum_{k=1}^{m} NW_{\mathrm{Litz}}. \tag{19}$$

It can be seen that the biggest reduction in leakage inductance at high frequency occurs when the number of layers becomes relatively large; in this condition, the proximity factor determines the reduction percentage of leakage inductance. Finally, the total leakage inductance is obtained by substituting $W_{\mathrm{pri/sec\_Litz}}$ in (19) into (20), the interwinding leakage energy W_g and inter layer one $W_{\mathrm{pri/sec\_ins}}$ are shown in (1) and (2), respectively.

$$L_\delta = \frac{2}{I_1^2}(W_g + W_{\mathrm{pri\_Litz}} + W_{\mathrm{sec\_Litz}} + W_{\mathrm{Pri\_ins}} + W_{\mathrm{sec\_ins}}). \tag{20}$$

In order to disclose the distribution of the leakage inductance of each part, a transformer with Litz wire winding is analyzed and the parameters are given in Table I. Note that the strand diameter D_s (0.1 mm) is chosen to be much smaller than the skin depth δ (0.661 mm) at chosen frequency so that the reduction effect of the leakage inductance within Litz wire is negligible. The leakage inductance distribution in the example transformer is shown in Fig. 8 with different interwinding distances. It can be seen that the leakage magnetic energy is largely stored in the interwinding insulation region, especially when this insulation distance is relatively large, and there is considerable leakage

TABLE I
WINDING STRUCTURE OF THE EXAMPLE TRANSFORMER

Core	CN-138*95*45*30	
Winding	Primary	Secondary
Number of layers	1	3
Diameter of Litz wire (D_{Litz})	4.9 mm	
Diameter of each strand (D_s)	0.1 mm	
Turns per layer (N)	20	
Inter-winding distance (d_{ins})	5, 10, 20 mm	
Inter-layer distance ($d_{ins1/2}$)	5 mm	
Distance between winding and core (d_{ins_core})	2 mm	
Frequency (f)	10 kHz	

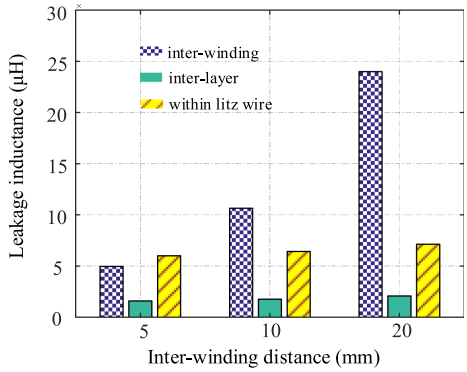

Fig. 8. Leakage energy distribution of the example transformer.

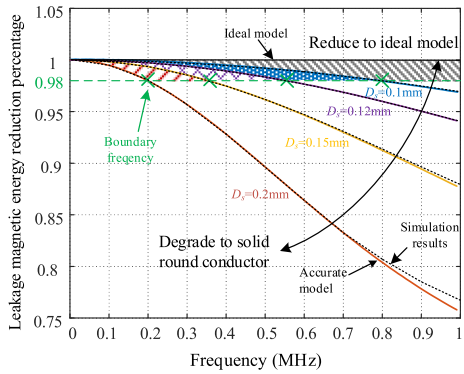

Fig. 9. Leakage magnetic energy reduction percentage of Litz wire with different strand diameters predicted by accurate model and numerical simulation (considering strand level proximity effect).

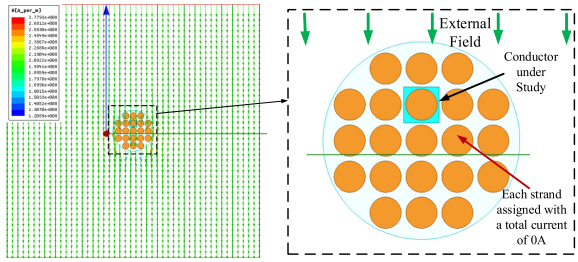

Fig. 10. FEA settings of the leakage magnetic energy reduction percentage (with external traverse time-varying magnetic field from 0 Hz to 1 MHz).

magnetic energy stored in Litz wire as well, which should not be neglected.

D. Relationship Between the Ideal Model and Accurate Model

A high-frequency transformer with Litz wire winding is less susceptible to the frequency effects compared with one using foil or solid round conductors, because generally the diameter of each strand is much smaller, causing a small penetration ratio, thus suppressing the reduction in the leakage inductance. The biggest deviation of an ideal model from accurate model occurs under the multilayer condition. The decline of leakage inductance at high frequency is characterized by the skin and proximity effect factors (γ_1 and γ_2), and the reduction percentage of the proximity factor is much stronger, as shown in Fig. 7. At the same time, It can be obtained from (19) that the proximity factor dominates the skin factor when the number of layer m becomes large. As a result, the biggest deviation of the ideal model from an accurate model occurs under the multilayer condition, in this condition, the proximity factor determines the reduction percentage of the leakage inductance in consequence. As a result, only the strand level proximity is taken into account in Fig. 9, which demonstrates the leakage inductance reduction percentage versus frequency with a filling factor of 0.6.

A numerical simulation is performed to validate the accurate analytical method. The FEA settings are shown in Fig. 10, a traverse external field is applied on the Litz wire. Note that a current excitation (type: solid) of 0 A is assigned to each strand, which guarantees that each strand will share equal current but will still be affected by a strand level proximity effect. A frequency range from 0 Hz to 1 MHz is performed to find out the leakage magnetic energy reduction percentage. The normalized results are shown in Fig. 9, represented by different dotted curves, which are in accordance with the analytical results (solid line). The slight deviation of FEA results of the leakage magnetic energy at high frequency is due to the distortion of the magnetic field near the strand.

As shown in Fig. 9, the accurate model is reduced to an ideal model when the diameter of Litz strand becomes smaller, and degraded to the solid round conductor model when the strand diameter becomes relatively large. The shadowed area represents the 2% maximum relative error region between the ideal model and the actual accurate model, the cross mark shows the boundary frequency, over which the tolerance of the ideal model is greater than 2%. For instance, when the diameter of Litz strand is 0.1 mm, the relative error of leakage energy in the Litz wire with the ideal model is less than 2% when the working frequency is lower than 800 kHz. Hence, the ideal model could be effective on the occasion where accuracy is not the first priority. However, when it comes to megahertz ranges, or under the circumstance where the conductor is twisted by the insulated wires with a diameter of larger than 0.2 mm, the actual model should be used to guarantee high accuracy.

III. PARAMETER SENSITIVITY ANALYSIS

According to the previous analysis, the model of leakage inductance in a high-frequency transformer is characterized by a large number of parameters. The influence of each parameter on the leakage inductance is different. Each individual parameter

has a degree of freedom in the optimization design process and a large number of parameters mean high-dimensional search space, leading to long computation time. Therefore, the influence of these parameters should be analyzed so that the more influential parameters on the leakage inductance will be taken into consideration and the other parameters could be fixed, reducing the computation time. In addition, when manufacturing the transformer, the variation of different parameters has different influence on overall leakage inductance. Hence, attention should be paid to those more sensitive parameters. However, it is difficult to estimate which of those parameters has high influence on the result in a highly complex and nonlinear model. A variance-based sensitivity analysis is a form of a global sensitivity analysis method, it decomposes the variance of the output of the model or system into fractions which can be attributed to inputs or sets of inputs. In this section, a Sobol-based sensitivity analysis is carried out in order to determine the influence of each parameter on the leakage inductance.

Any model can be considered as a function $Y = f(\mathbf{X})$, where $\mathbf{X}$ is a vector of independent random variables $\{x_1, x_2, \ldots x_d\}$ distributed uniformly in unit hyperspace and Y is the model output. Decomposition of variance is made as follows:

$$V = \mathrm{Var}(Y) = \sum_i V_i + \sum_i \sum_{j>i} V_{ij} + \cdots + V_{1,2,\ldots,d}$$
$$V_i = \mathrm{Var}(\mathrm{E}(Y\,|x_i\,))$$
$$V_{ij} = \mathrm{Var}(\mathrm{E}(Y\,|x_i\,, x_j)) - V_i - V_j \tag{21}$$

where E denotes the expected value and Var represents the variance. The $x_{\sim \mathrm{i}}$ notation indicates the set of all variables except x_i, and this decomposition shows the attribution of each input. Then the first-order effect index (main effect index) is defined as follows:

$$S_i = \frac{V_i}{\mathrm{Var}(Y)}. \tag{22}$$

The first-order index measures the effect of varying x_i alone, with other input parameters fixed to their average value. The large value of S_i shows that changing the corresponding parameter alone has great influence on the output, in this case, the leakage inductance. But the small value of S_i can still have an influence on the leakage inductance due to its interactions with other parameters [30]. The total effect index is defined as follows:

$$S_T = \sum_{S=1}^{d} \sum_{i_1, i_2, \ldots, i_s} S_1, i_2, \ldots, i_s. \tag{23}$$

The total effect index S_T measures the contribution to the output variance of x_i including all variances caused by its interactions. The small value of S_T indicates the parameter is unimportant and dispensable, and could be fixed in the expression.

The variance-based sensitivity analysis in two practical cases is carried out for the example transformer in Table I.

Case 1: Parameters are varied in a large but practical range with a uniform distribution. This could assess which parameters influence the leakage inductance the most, and those less influential parameters could be fixed when designing the transformer with a desired leakage inductance.

TABLE II
VARIANCE RANGE OF PARAMETERS IN SENSITIVITY ANALYSIS

Variables	*Case 1* (Uniform Distribution)	*Case 2* (Normal Distribution)
Litz wire Diameter (D_{Litz})	4~6mm	4.85~5.15mm (σ=1%)
Core-winding distance(d_{ins_core})	1~10mm	4.5~5.5mm (σ=3.33%)
Inter-layer distance ($d_{ins1/2}$)	1~10mm	4.5~5.5mm (σ=3.33%)
Inter-winding distance (d_{ins})	1~20mm	9~11mm (σ=3.33%)
Turns per layer (N)	15~30	20 (No error)

Case 2: Parameters are varied in a small range with a normal distribution (Gauss distribution). This could access the error occurred in practical manufacturing of the transformer, and extra attention should be paid to controlling those sensitive parameters, thus error could be minimized.

The variance range of the transformer variables is given in Table II, note that they are all in accordance with a practical situation (i.e., in *Case 1*, the range of N is 15–30, D_{Litz} is 4–6 mm to guarantee a reasonable working magnetic and current density, thus controlling other design objectives under a reasonable range.)

Several algorithms [Standard Sobol, Fourier amplitude sensitivity test (FAST), Saltelli, and Improved Sobol] [31]–[34] are implemented to guarantee reliability. The difference of these methods lies in that, as an improvement to the Standard Sobol [31], Saltelli *et al*. [32] implement a single-loop Monte Carlo method in random sampling process and FAST algorithm [33] combine FAST and random balanced design in order to achieve computational efficiency, the improved Sobol method [34] improves overall accuracy in the small sensitivity indices case. Fig. 11 shows the results of these sensitivity analysis. It should be noticed that, in the described single primary winding layer transformer, the distance between layers in the primary winding d_{c1} does not exist. So d_{ins1} can be viewed as an algorithm testing parameter and its value should be zero.

It can be seen from *case 1* in Fig. 11 that the interwinding distance d_{ins}, representing the leakage energy stored in insulation region between the primary and secondary windings, is the most influential parameter in the leakage inductance with an influence index of 0.5–0.6. Although this distance is linked with mean magnetic length, varying d_{ins} would have limited influence on other loss related design objectives, which makes it a perfect variable in changing the leakage inductance. The turns of conductor per layer N is the second major influential parameter in determining the leakage inductance. However, N is directly linked with the maximum magnetic flux density B_m, which means that the large variation of N could cause undesired and suboptimized core loss and even magnetic saturation, so attention should be paid to changing N. Although the leakage energy stored by Litz wire is significant, the practical range of D_{Litz} is constrained to a relatively small range. As a result, varying D_{Litz} in its reasonable range has limited influence. The distance between layers in the same winding $d_{ins1/2}$, representing the energy stored in winding layers, and the distance between primary winding and core, affecting magnetic flux length, have negligible influence on the total leakage inductance and could be fixed to reduce searching space in the optimization design.

Fig. 12 shows the leakage inductance versus variation of parameters. Fig. 12(a) shows the leakage inductance with the

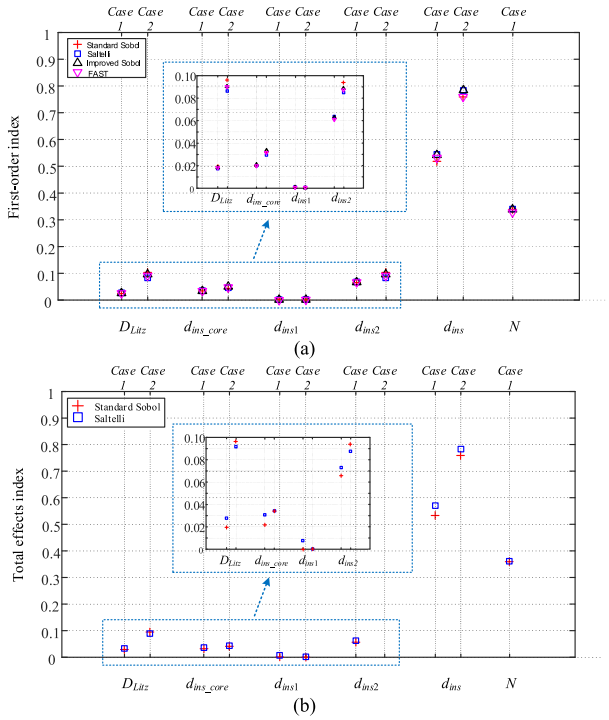

Fig. 11. Sensitivity index predicted by different algorithms of transformer structural parameters. *Case* 1: uniform distribution (large range); *case* 2: normal distribution (small range) (including diameter of Litz wire D_{Litz}, insulation distance between core and winding $d_{\mathrm{ins\_core}}$, interlayer distance in primary winding and secondary winding, respectively, d_{ins1} and d_{ins2}, insulation distance between primary and secondary winding d_{ins}, and number of turns per layer *N*). (a) First-order index (main effect). (b) Total effect index.

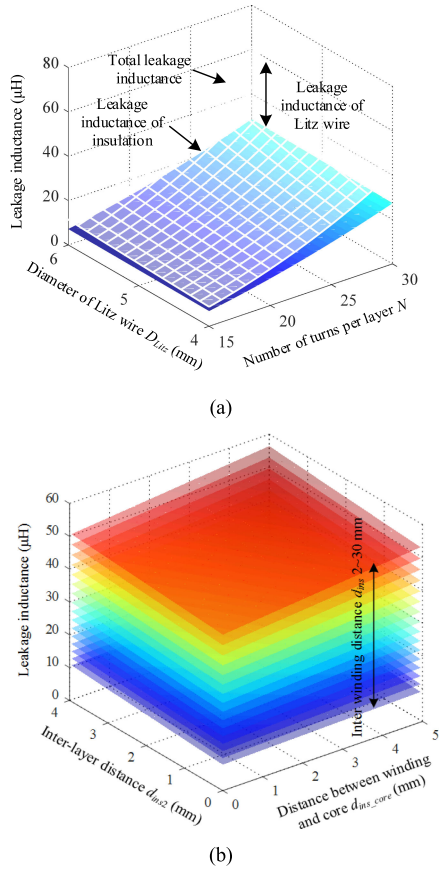

Fig. 12. Influence on leakage inductance. (a) Variation of number of turns per layer and diameter of Litz wire. (b) Alteration of insulation distance.

variation of number of turns per layer and the diameter of Litz wire. The lower plane represents the energy stored in air and insulation, and the upper plane represents the variation of overall leakage inductance. It can be seen that both the two parameters have considerable influence on the leakage inductance.

From Fig. 12(b), it is clear that the distance between the primary winding and the core has negligible influence on the leakage inductance, in spite of its effect on magnetic flux path. For the fact that the portion of energy stored in interlayer insulation is relatively small, the influence of interlayer distance is also small. Finally, varying the interwinding distance is the most reliable way to obtain a desired leakage inductance because the influence of this distance is prominent quasi linear, and it has negligible influence on winding loss and core loss.

The result of sensitivity analysis *case* 2 in Fig. 11 clearly shows that, as the most sensitive parameter (with a sensitivity index of 0.7–0.8), deviation of d_{ins} when manufacturing the transformer could cause a large relative error in overall leakage inductance. Small error in other parameters such as D_{Litz}, $d_{ins1/2}$, $d_{\mathrm{ins\_core}}$ (with sensitivity indices $\leq$0.1) normally would not cause inaccuracy in overall leakage inductance. Fig. 13 shows the relative error of the leakage inductance of the example transformer caused by manufacturing uncertainties of d_{ins} (normal distribution), the values of other parameters are fixed, as defined in Table I. For instance, if the interwinding distance of the transformer fails to be precise during manufacturing, suppose

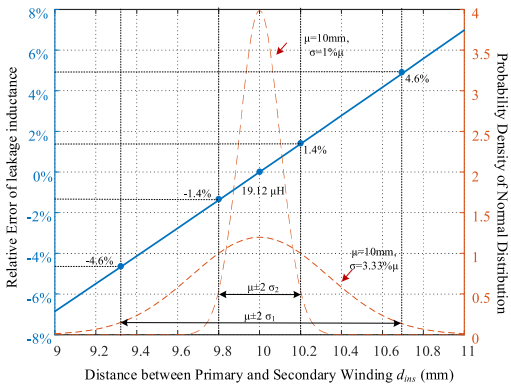

Fig. 13. Relative error of leakage inductance of the example transformer presented in Table I caused by manufacturing uncertainties of d_{ins} (normal distribution).

there is a standard deviation of 3.33% in d_{ins} ($\mu\pm3\sigma$: 9–11 mm), the biggest relative error of leakage inductance would be $\pm$6.4%, at the same time, the probability of relative error smaller than 4.6% is 95.5% ($\mu\pm2\sigma$: 9.4–10.6 mm). If the standard deviation of d_{ins} is smaller, say 1%, the accuracy of leakage inductance will improve a lot and the tolerance of leakage inductance is much likely to be less than 1.4%. Therefore, controlling the relative error of d_{ins} deserves extra caution during manufacturing.

TABLE III
STRUCTURAL PARAMETERS OF THE TRANSFORMER PROTOTYPES

Prototype	Transformer-I		Transformer-II	
Core	EE 110 Ferrite			
Window height(h_c)	75 mm			
Winding height(h_w)	70 mm			
Winding	Primary	Secondary	Primary	Secondary
Number of Layers (m)	1	1	1	3
Diameter of Litz wire (D_{Litz})	4.90 mm		2.44mm	
Diameter of each strand (D_s)	0.1 mm		0.2mm	
Filling factor of Litz wire	0.42		0.54	
Turns per layer (N)	14		26	
Inter-winding distance (d_{ins})	5 mm		3 mm	
Inter-layer distance ($d_{ins1/2}$)	/		0.05 mm	
Distance between Winding and Core (d_{ins_core})	2 mm		2 mm	

(a) (b) (c)

Fig. 14. Leakage inductance mesurement. (a) Transformer-I. (b) Transformer-II. (c) E5061B Network analyzer.

IV. EXPERIMENTAL VERIFICATION

In order to verify the accuracy of the proposed model, two shell-type transformer prototypes are built for verification and the structural parameters are presented in Table III. Both primary and secondary windings of the transformers are wound around the middle core column. The two prototypes are shown in Fig. 14.

The Agilent E5061B network analyzer is used to measure the leakage inductance of the transformer versus frequency. The inductance–frequency curve of a small piece of Litz wire is measured as a correction to the system error of the network analyzer. The final transformer leakage inductance is then obtained by subtracting the wire correction value from the transformer measured value.

Fig. 15(a) shows the leakage inductance of transformer-I within a frequency range of 0–2 MHz and Fig. 15(b) demonstrates its variation within 800 kHz range. Fig. 16(a) shows the leakage inductance of transformer-II within a frequency range of 0–2 MHz and Fig. 16(b) demonstrates its variation within 300 kHz range. Note that when the secondary winding is shorted, the capacitive current could cause a measurement error in the measured leakage inductance near the parallel resonance point. However, the resonance frequency (25.95 MHz for transformer-I and 14.54 MHz for transformer-II) is well above the frequency range analyzed in the article. The influence of capacitive current on the measured leakage inductance at 0–2 MHz is negligible (in this condition, stray capacitance is parallel to the leakage inductance, maximum measurement error caused by parallel capacitive current is around 0.6% for transformer-I and 1.8% for transformer-II).

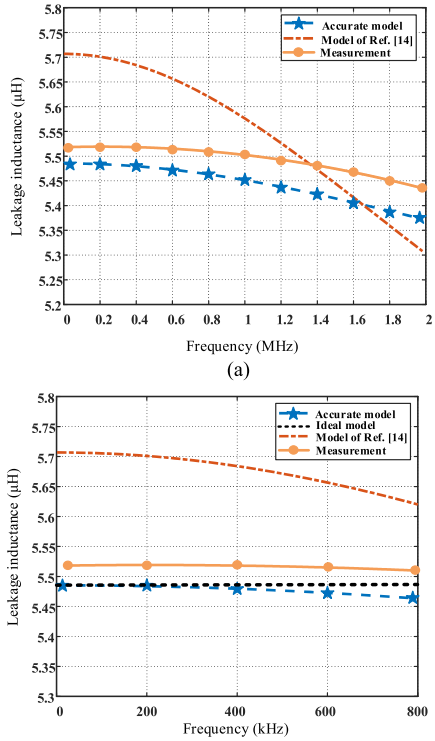

Fig. 15. Comparisons of leakage inductances of transformer-I among measurement, accurate model, and modified Dowell model (with correction of equivalence diameter). (a) 0–2 MHz range. (b) 0–800 kHz range.

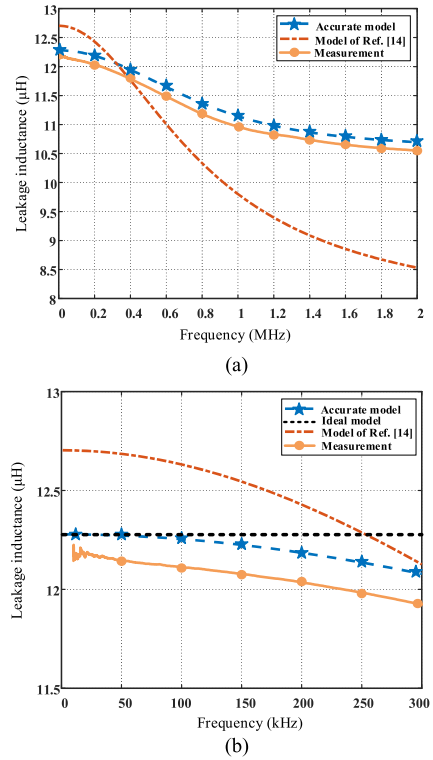

Fig. 16. Comparisons of leakage inductances of transformer-II among measurement, accurate model, and modified Dowell model (with correction of equivalence diameter). (a) 0–2 MHz range. (b) 0–300 kHz range.

Results show that there is a reduction in the leakage inductance at high frequency. For transformer-I, experimental results show that its leakage inductance drops from 5.52 μH at 10 kHz to around 5.43 μH at 2 MHz and that of transformer-II drops from 12.2 μH to 10.5 μH at 2 MHz, this is due to the decrease of leakage energy inside the Litz wire conductor. The reduction of the leakage inductance in transformer-II is more prominent, this is mainly due to the fact that the diameter of the Litz strand in transformer-II is larger, causing a relatively strong proximity effect. How much the leakage inductance will fall depends on the relative size of the Litz strand diameter D_s and skin depth δ at a given frequency. For transformer-I and transformer-II, it shows that when D_s is smaller than skin depth, the reduction in leakage inductance will be negligible. When the operating frequency increases and D_s becomes two times larger than the skin depth, the frequency effect on leakage inductance should be considered. The diameter of the Litz bundle D_{Litz}, which is directly linked with the number of strands when strand diameter is fixed, on the other hand, has very limited influence on the frequency effect of the leakage inductance in a fully twisted Litz wire.

It can be seen that the proposed method yields high accuracy for both transformer prototypes in whole frequency range. In addition, the analytical result of an ideal model (frequency effect neglected) is almost as precise as the accurate model in low-frequency range (within 800 kHz range for the diameter of Litz strand is 0.1 mm and within 200 kHz range for the diameter of the Litz strand is 0.2 mm). The model in [14] (with correction in strand diameter) overestimates the leakage inductance in low frequency, and its remarkable reduction in the leakage inductance is mainly caused by neglecting the influence of Litz wire's filling factor.

V. Conclusion

This article proposes a new analytical approach to accurately calculate the leakage inductance in a wide frequency range. Alternating the distance between the primary and secondary windings is the most effective way to obtain a desired leakage inductance due to its least effect on winding loss and core loss. At the same time, as the most sensitive parameter, precisely controlling the tolerance of interwinding distance is crucial to reduce the relative error of the leakage inductance when manufacturing the transformer. Although reduction in the leakage inductance is predicted in the accurate model with the increase of an operation frequency, the ideal model could be time-saving in the optimization design process with negligible compromise in the accuracy when the operation frequency is relatively low, or when implementing very fine strands at high frequency (which is a necessity when the conducting current is high). The accurate frequency dependent model ought to be used in an occasion where the Litz strand diameter becomes two times larger than skin depth, this usually occurs when the operating frequency is in the megahertz range, using the Litz wire with a strand diameter around 0.1 mm (tradeoff between winding loss and cost), or under the circumstance where the conductor is twisted by a surface insulated wire with a diameter of more than 0.2 mm. The leakage inductance of the transformer implementing the Litz wire is less susceptible to frequency change than its counterpart (foil, solid round conductor), which makes it a perfect choice for resonant converter with frequency control.

References

[1] M. A. Bahmani and T. Thiringer, "Accurate evaluation of leakage inductance in high-frequency transformers using an improved frequency-dependent expression," *IEEE Trans. Power Electron.*, vol. 30, no. 10, pp. 5738–5745, Oct. 2015.

[2] M. A. Bahmani, T. Thiringer, and H. Ortega, "An accurate pseudoempirical model of winding loss calculation in HF foil and round conductors in switchmode magnetics," *IEEE Trans. Power Electron.*, vol. 29, no. 8, pp. 4231–4246, Aug. 2014.

[3] B. Li, Q. Li, and F. C. Lee, "A novel PCB winding transformer with controllable leakage integration for a 6.6kW 500 kHz high efficiency high density bi-directional on-board charger," in *Proc. IEEE Appl. Power Electron. Conf. Expo.*, Tampa, FL, USA, 2017, pp. 2917–2924.

[4] J. Biela and J. W. Kolar, "Design of high power electromagnetic integrated transformers by means of reluctance models and a structured survey of leakage paths," presented at the 35th IEEE Power Electron. Spec. Conf., Aachen, Germany, Jun. 20–25, 2004.

[5] K. Wang, Z. Qi, F. Li, L. Wang, and X. Yang, "Review of state-of-the-art integration technologies in power electronic systems," *CPSS Trans. Power Electron. Appl.*, vol. 2, no. 4, pp. 292–305, Dec. 2017.

[6] A. Q. Huang, "Medium-voltage solid-state transformer: Technology for a smarter and resilient grid," *IEEE Ind. Electron. Mag.*, vol. 10, no. 3, pp. 29–42, Sep. 2016.

[7] F. Briz, M. Lopez, A. Rodriguez, and M. Arias, "Modular power electronic transformers: Modular multilevel converter versus cascaded H-bridge solutions," *IEEE Ind. Electron. Mag.*, vol. 10, no. 4, pp. 6–19, Dec. 2016.

[8] Z. Ouyang, J. Zhang, and W. G. Hurley, "Calculation of leakage inductance for high-frequency transformers," *IEEE Trans. Power Electron.*, vol. 30, no. 10, pp. 5769–5775, Oct. 2015.

[9] J. Yang, J. Liu, J. Zhang, N. Zhao, Y. Wang, and T. Q. Zheng, "Multirate digital signal processing and noise suppression for dual active bridge DC–DC converters in a power electronic traction transformer," *IEEE Trans. Power Electron.*, vol. 33, no. 12, pp. 10885–10902, Dec. 2018.

[10] W. T. McLyman, *Transformer and Inductor Design Handbook*, 4th ed. Boca Raton, FL, USA: CRC Press, 2011.

[11] S. R. Thondapu, M. B. Borage, Y. D. Wanmode, and P. Shrivastava, "Improved expression for estimation of leakage inductance in E core transformer using energy method," *Adv. Power Electron.*, vol. 2012, 2012, Art. no. 635715.

[12] W. G. Hurley and D. J. Wilcox, "Calculation of leakage inductance in transformer windings," *IEEE Trans. Power Electron.*, vol. 9, no. 1, pp. 121–126, Jan. 1994.

[13] F. Lv *et al.*, "Calculation and correction method for leakage inductance of high-power medium-frequency transformer," *High Voltage Eng.*, vol. 42, no. 6, pp. 170–1707, Jun. 2016 (in Chinese).

[14] M. Mogorovic and D. Dujic, "Medium frequency transformer leakage inductance modeling and experimental verification," in *Proc IEEE Energy Convers. Congr. Expo.*, Cincinnati, OH, USA, 2017, pp. 419–424.

[15] W. Tan, X. Margueron, L. Taylor, and N. Idir, "Leakage inductance analytical calculation for planar components with leakage layers," *IEEE Trans. Power Electron.*, vol. 31, no. 6, pp. 4462–4473, Jun. 2016.

[16] J. Zhang, Z. Ouyang, M. C. Duffy, M. A. E. Andersen, and W. G. Hurley, "Leakage inductance calculation for planar transformers with a magnetic shunt," *IEEE Trans. Ind. Appl.*, vol. 50, no. 6, pp. 4107–4112, Nov./Dec. 2014.

[17] H. Rossmanith and E. Stenglein, "Prediction of the leakage inductance in high frequency transformers," in *Proc. 18th Eur. Conf. Power Electron. Appl.*, Karlsruhe, Germany, 2016, pp. 1–10.

[18] V. S. Duppalli and S. Sudhoff, "Computationally efficient leakage inductance calculation for a high-frequency core-type transformer," in *Proc. IEEE Electr. Ship Technol. Symp.*, Arlington, VA, USA, 2017, pp. 635–642.

[19] F. C. Lee, Q. Li, Z. Liu, Y. Yang, C. Fei, and M. Mu, "Application of GaN devices for 1 kW server power supply with integrated magnetics," *CPSS Trans. Power Electron. Appl.*, vol. 1, no. 1, pp. 3–12, Dec. 2016.

[20] Q. Huang and A. Q. Huang, "Review of GaN totem-pole bridgeless PFC," *CPSS Trans. Power Electron. Appl.*, vol. 2, no. 3, pp. 187–196, Sep. 2017.

[21] C. R. Sullivan, "Optimal choice for number of strands in a litz-wire transformer winding," *IEEE Trans. Power Electron.*, vol. 14, no. 2, pp. 283–291, Mar. 1999.
[22] F. Tourkhani and P. Viarouge, "Accurate analytical model of winding losses in round Litz wire windings," *IEEE Trans. Magn.*, vol. 37, no. 1, pp. 538–543, Jan. 2001.
[23] X. Nan and C. R. Sullivan, "An equivalent complex permeability model for Litz-wire windings," *IEEE Trans. Ind. Appl.*, vol. 45, no. 2, pp. 854–860, Mar./Apr. 2009.
[24] D. C. Meeker, "An improved continuum skin and proximity effect model for hexagonally packed wires," *J. Comput. Appl. Math.*, vol. 236, no. 18, pp. 4635–4644, 2012.
[25] I. Villar, "Multiphysical characterization of medium-frequency power electronic transformers," Ph.D. dissertation, Ind. Electron. Lab., EPFL Lausanne, Lausanne, Switzerland, 2010.
[26] J. Acero, R. Alonso, J. M. Burdio, L. A. Barragan, and D. Puyal, "Frequency-dependent resistance in Litz-wire planar windings for domestic induction heating appliances," *IEEE Trans. Power Electron.*, vol. 21, no. 4, pp. 856–866, Jul. 2006.
[27] J. A. Ferreira, "Improved analytical modeling of conductive losses in magnetic components," *IEEE Trans. Power Electron.*, vol. 9, no. 1, pp. 127–131, Jan. 1994.
[28] J. Lammeraner and M. Stafl, *Eddy Currents*. Cleveland, OH, USA: CRC Press, 1966.
[29] M. Perry and T. Jones, "Eddy current induction in a solid conducting cylinder with a transverse magnetic field," *IEEE Trans. Magn.*, vol. 14, no. 4, pp. 227–232, Jul. 1978.
[30] L. J. Opalski, "Efficient global sensitivity analysis method for models of systems with functional outputs," in *Proc. Eur. Conf. Circuit Theory Des.*, Trondheim, Norway, 2015, pp. 1–4.
[31] I. M. Sobol, "Global sensitivity indices for nonlinear mathematical models and their Monte Carlo estimates," *Math. Comput. Simul.*, vol. 55, pp. 271–280, 2001.
[32] A. Saltelli *et al.*, *Global Sensitivity Analysis: The Primer*. Hoboken, NJ, USA: Wiley, 2008.
[33] S. Tarantola, D. Gatelli, and T. A. Mara, "Random balance designs for the estimation of first order global sensitivity indices," *Rel. Eng. Syst. Saf.*, vol. 91, no. 6, pp. 717–727, 2006.
[34] I. M. Sobol and E. E. Myshetskaya, "Monte Carlo estimators for small sensitivity indices," *Monte Carlo Methods Appl.*, vol. 13. no. 5/6, pp. 455–465, 2008.

Ke Zhang was born in Jiangsu, China, in 1994. He received the B.S. degree in electrical engineering from the Changshu Institute of Technology, Jiangsu, China, in 2017. He is currently working toward the M.S. degree in electrical engineering with Southeast University, Nanjing, China.

His research interests include high-frequency transformer model and design, and its medium-voltage dc applications including power electronic transformer and energy router.

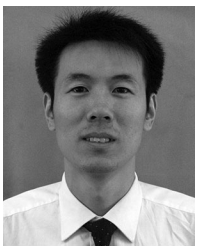

Wu Chen (S'05–M'12–SM'17) was born in Jiangsu, China, in 1981. He received the B.S., M.S., and Ph.D. degrees in electrical engineering from the Nanjing University of Aeronautics and Astronautics, Nanjing, China, in 2003, 2006, and 2009, respectively.

From 2009 to 2010, he was a Senior Research Assistant with the Department of Electronic Engineering, City University of Hong Kong, Kowloon, Hong Kong. From 2010 to 2011, he was a Postdoctoral Researcher with Future Electric Energy Delivery and Management Systems Center, North Carolina State University, Raleigh, NC, USA. Since September 2011, he has been an Associate Research Fellow with the School of Electrical Engineering, Southeast University, Nanjing, China, where he has been a Professor since 2016. His main research interests include soft-switching converters, power delivery, and power electronic system integration.

Dr. Chen serves as an Associate Editor for the IEEE TRANSACTIONS ON INDUSTRIAL ELECTRONICS, *Journal of Power Electronics*, and *CPSS Transactions on Power Electronics and Applications*.

Xiaopeng Cao was born in Gansu, China, in 1990. He received the B.S. degree in electronic engineering from Central South University, Hunan, China, in 2015, and the M.S. degree in electrical engineering from Southeast University, Nanjing, China.

His main research interest focuses on power electronic transformers.

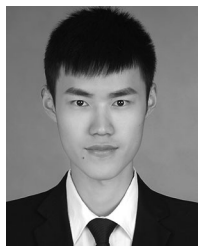

Pengpeng Pan was born in Jiangsu, China, in 1996. He received the B.S. degree in electrical engineering from Nanjing Normal University, Jiangsu, China, in 2017. He is currently working toward the M.S. degree in electrical engineering with Southeast University, Nanjing, China.

His research interests include the virtual synchronous generator and the stability assessment and control strategy of medium and low voltage dc distribution power system.

Syed Waqar Azeem was born in Kohat, Pakistan, in 1989. He received the B.S. degree in electrical engineering from Northwestern Polytechnical University, Xi'an, China, and the M.S. degree from Xi'an Jiaotong University, Xi'an, in 2013 and 2016, respectively. He is currently working toward the Ph.D. degree with Southeast University, Nanjing, China.

His research interests include three-level converters, soft-switching techniques, and high-power high-voltage dc/dc converters.

Guangyao Qiao was born in Chongqing, China, in 1981. He received the B.S. degree in electrical engineering from Beijing Jiaotong University, Beijing, China, in 2006, and the M.Sc. degree in power electronics from China Electric Power Research Institute (CEPRI), Beijing, in 2009.

Since 2009, he has been working with the Department of Power Electronics, CEPRI, and Global Energy Interconnection Research Institute, Beijing, China. His current interests include FACTS system design and its application.

Fujin Deng (S'10–M'13–SM'19) received the B.Eng. degree in electrical engineering from the China University of Mining and Technology, Jiangsu, China, in 2005, the M.Sc. degree in electrical engineering from Shanghai Jiao Tong University, Shanghai, China, in 2008, and the Ph.D. degree in energy technology from Aalborg University, Aalborg, Denmark, in 2012.

In 2017, he joined Southeast University, Nanjing, China, where he is currently a Professor with the School of Electrical Engineering. From 2013 to 2015 and from 2015 to 2017, he was a Postdoctoral Researcher and an Assistant Professor, respectively, with the Department of Energy Technology, Aalborg University. His main research interests include wind power generation, multilevel converters, high-voltage direct current technology, dc grid, and offshore wind farm-power systems dynamics.